1997 Kronotsky earthquake and tsunami and their predecessors, Kamchatka, Russia

Joanne Bourgeois[1], Tatiana K. Pinegina[2]

[1]Department of Earth and Space Sciences, University of Washington, Seattle, WA 98195-1310, USA
[2]Institute of Volcanology and Seismology, FEB RAS, 9 Piip Boulevard, Petropavlovsk-Kamchatsky, 683006, Russia

Correspondence to: Joanne Bourgeois (jbourgeo@uw.edu)

Abstract. The northern segment of the Kamchatka subduction zone (KSZ) experienced three tsunamigenic earthquakes in the 20th century (Feb 1923, April 1923, Dec 1997), events that help us better understand the behavior of this segment. Characterizing these historical earthquakes and tsunamis in turn contributes to interpreting the prehistoric record, which is necessary to evaluate recurrence intervals for such events. A particular focus of this study is the nature and location of the 5 December 1997 Kronotsky rupture as elucidated by tsunami runup in southern Kamchatsky Bay. Some studies have characterized the subduction zone off Kronotsky Peninsula as less seismogenic, as indicated by gravity-anomaly analyses, and have placed the 1997 rupture south of the promontory. However, tsunami runup north of the peninsula, as evidenced by our mapping of tsunami deposits, requires the rupture to extend farther north. Previously reported runup (1997 tsunami) on Kronotsky Peninsula was no more than 2-3 m, but our studies indicate tsunami heights for at least 50 km north of the peninsula, ranging from 3.4 to 9.5 m (average 6.1 m), exceeding beach ridge heights of 5.3 to 8.3 m (average 7.1 m). For the two 1923 tsunamis, we cannot distinguish their deposits in southern Kamchatsky Bay, but they are in sum more extensive than the 1997 deposit. A reevaluation of the April 1923 earthquake (and its tsunami) suggests that its moment magnitude should be revised upward to Mw ~8. This revision makes the two 1923 events more like a pair, with the 1997 earthquake filling a gap between them. Deeper in time, the 1700-year prehistoric record of tsunamis in southern Kamchatsky Bay indicates that during this interval, there were no local events significantly larger than the 20th century earthquakes. Together, the historic and prehistoric record suggests a more northerly location of the 1997 rupture, a revision of the size of the April 1923 earthquake, and agreement with previous work suggesting the northern KSZ ruptures in smaller sections than the southern KSZ. The latter conclusion requires caution, however, as we continue to learn that our historic and even pre-historic records of earthquakes and tsunamis is limited, in particular as applied to hazard analysis. This study is a contribution to our continued efforts to understand tectonic behavior around the northern Pacific and in subduction zones, in general.

Key words: Kamchatka, subduction zone, 1997 Kronotsky earthquake, 1997 Kronotsky tsunami, Kamchatsky Bay, paleotsunami, paleoseismology

[copyright statement]

1 Introduction

34
35   References to the modest or small tsunami of 15 December 2006 central Kurils (Ammon et al., 2008; Liu,
36 2009), when in fact this tsunami generated an average of 9.6 m runup over an along-rupture length of 390 km
37 (MacInnes et al., 2009), remind us that without post-tsunami or tsunami-deposit surveys, remote spots in the world
38 may experience large events without a written record. The case of the 5 December 1997 tsunami following the Mw
39 7.7-7.9 Kronotsky earthquake (Fig. 1, Fig. 2), however, is even more complex historically, because there *was* a post-
40 tsunami survey quickly following (Zayakin and Pinegina, 1998), though of limited extent. The local tide-gage record
41 for this 1997 tsunami is also incomplete, and deep-water pressure recorders deployed at the time were not positioned
42 to get distinctive recordings from a tsunami originating near Kronotsky Cape (Bourgeois and Titov, 2001). The
43 earthquake and tsunami occurred in the dark of a December night in an area with no permanent settlements.

44

Figure 1. General tectonic setting and locations. **Upper left**: Major topography of and bathymetric features around Kamchatka. **Lower left**: locations of sites mentioned in text and tables. **Right**: Interpreted rupture locations of 20th century tsunamigenic (except *1923.II.24*) earthquakes along the Kamchatka portion of the Kuril-Kamchatka subduction zone (modified from Gusev , 2004, Fig. S1; Martin et al., 2008). The rupture area of the 1997 earthquake varies in different analyses, one of the subjects of this (our) paper; also discussed are the 1923 earthquakes. PK = Petropavlovsk-Kamchatsky; UK = Ust-Kamchatsk; BI = Bering Island.
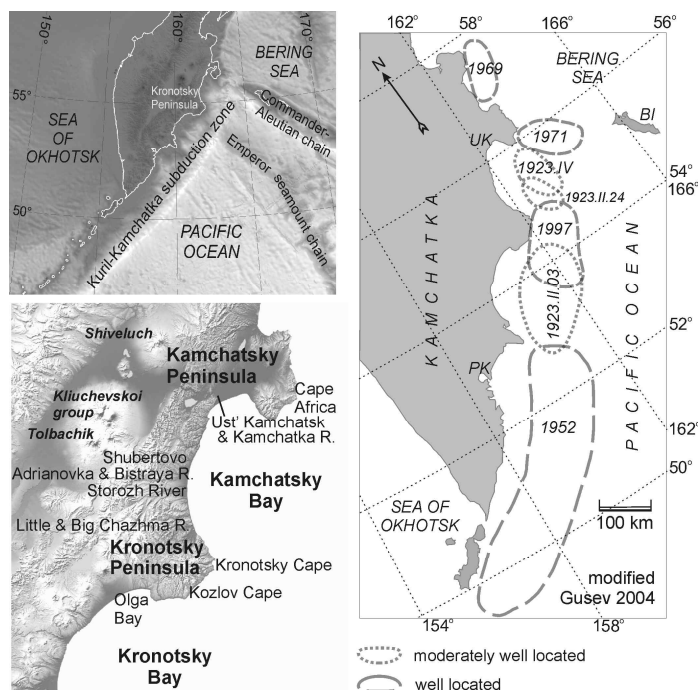
69   In the summer of 2000, we conducted a field survey for historical and paleo- tsunami deposits in south
70 Kamchatsky Bay (Fig. 1), north of Kronotsky Peninsula. We expected to find evidence of historical Kamchatka
71 tsunamis such as 1923 (Table 1; Table S1), but not for 1997 Kronotsky because on the southern Kronotsky
72 Peninsula, the post-tsunami survey found evidence of quite limited runup. Thus we were surprised to find a sand
73 layer just at the surface, covered only by plant debris such as grass and leaves, distributed much as we have come to
74 expect of tsunami deposits, and at elevations of 5 m or more above sea level. No alternative other than a tsunami
75 from the 1997 earthquake and its aftermath could explain the layer and its distribution.

76   The implications of this case, where an earthquake was analyzed without full knowledge its tsunami, are

77   several. First, the fact that there was runup greater than that reported by a post-tsunami survey changes our view of

78   the tsunami as well as of the earthquake. Further, the size of the tsunami, based on its deposits and a corroborating

79   eyewitness account (acquired in 2001), constrains the rupture characteristics of this earthquake. The tsunamigenic

80   portion of this earthquake was in a "gap" between two 1923 tsunamigenic earthquakes, at least one of which was

81   locally larger than 1997.

82   This recent historical tsunami also helps us interpret earlier historical and well as prehistoric earthquakes

83   and tsunamis along the northernmost part of the Kuril-Kamchatka subduction zone. Tsunamis originating from this

84   region commonly have an impact not only locally but also on Hawaii, as did the February 1923 tsunami, and in

85   some cases even on the western coast of the Americas, as did the 2006 central Kurils tsunami.

86

87   **2 Background**

88   **2.1 The 1997 Kronotsky earthquake**

89   On 5 December 1997 at 23:26:51 local time (11:26:51 UTC), a large earthquake (Mw 7.7-7.9; we use 7.8)

90   shook the region of the Kronotsky Peninsula, Kamchatka, Russia (Fig. 1, Fig. 2; Gordeev et al., 1998). The

91   earthquake was characterized by a typical foreshock-mainshock-aftershock sequence (Gusev et al., 1998; Fedotov et

92   al., 1998; Balakina, 2000; Zobin and Levina, 2001; Kuzin et al. 2007; Slavina et al., 2007). Most studies of the

93   earthquake calculate a moment magnitude of 7.8 for the energy released in the first 60-80 seconds of the main

94   rupture (e.g., Zobin and Levina, 2001). Gusev and Shumilina (2004), in reassessing many Kamchatka earthquakes,

95   assign Mw 7.9 to Kronotsky 1997. In addition to the mainshock, and using GPS measurements, Gordeev et al.

96   (2001) calculate Mw 7.7 for deformation in the *pre-seismic* half month, and approximately Mw 7.9 for *post-seismic*

97   deformation; Bürgmann et al. (2001) calculate Mw 7.7 of (*post-seismic*) aseismic energy release in the 2 months

98   following the mainshock, also based on GPS data.

99   The locations of the mainshock and of any slip concentration for this earthquake have not been well

100   resolved, and with one early exception (Sohn, 1998), locators have not used tsunami data. Based on seismic data,

101   the locations of foreshocks and the mainshock/epicenter (Fig. 2) are in the northern part of the interpreted rupture

102   area. A number of analytical locations of the mainshock lie under the NE Kronotsky Peninsula (Fig. 2; Table S2).

103   Some analyses interpret the rupture to have propagated NE to SW (Petukhin et al., 1998), deepening toward the SW.

104   Gusev (2004) maps the entire aftershock zone as part of the 1997 event (Fig. 1). On the other hand, the linear zone

105   of aftershocks in the SW (Fig. 2) has been interpreted to be a separate stress zone (Kuzin et al., 2007) potentially

106   along a separate transverse fault (Slavina et al., 2007). In an analysis focused on GPS data, Bürgmann et al. (2001)

107   place the majority of the primary rupture energy in the southern half of the aftershock zone.

108

Figure 2. Foreshocks (3-5 Dec 1997), mainshock and aftershocks of the 5 December 1997 Kronotsky earthquake (Gusev et al., 1998). Plotted foreshocks and MKZ aftershocks include only cases where P and S arrivals could be read from records of the nearest station, MKZ. Locations of epicenters and hypocenters are from various analyses, both local and farfield as reported from the International Seismological Center (Table S2). Slavina et al. (2007) interpret the southwestern aftershock activity to be on a separate, transverse fault; Kuzin et al. (2007) also interpret the SW portion of the (extended) aftershock region to be a separate stress zone
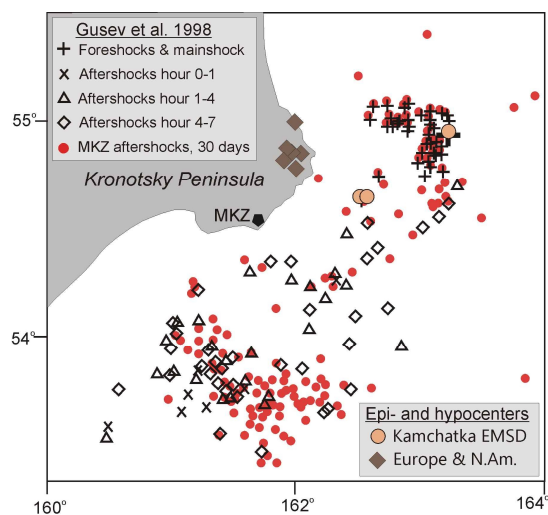
2.2 The recorded 1997 Kronotsky tsunami

The most complete contemporary record of the 1997 Kronotsky tsunami is from far-field tide gages. Both proximal tide gages, in Ust' Kamchatsk and in Nikolskoe (Bering Island) (Fig. 1), were not functioning when the tsunami arrived. The Petropavlovsk-Kamchatsky gage is very protected and shows a wave train with an amplitude of about 0.01 m (Zayakin and Pinegina, 1998). The tide gage at Nikolskoye resumed recording after the first 10 hours of the tsunami, with a few cm of amplitude remaining (Zayakin and Pinegina, 1998). The far-field tsunami had tide-gage amplitudes in Alaska/Aleutians and Hawaii in line with other tsunamis traveling to Hawaii from the Russian Far East (Table S3; Fig. S4). The tsunami was recorded on at least 12 tide gages (Table S3), with the highest amplitude (half of wave height) of 0.3 m at Kahului, Maui, Hawaii. Deep-water pressure sensors deployed at that time in the north Pacific were all in tsunami shadows for this tsunami source, and in all cases, the modeled and measured tsunami was within the noise level of the buoys (Bourgeois and Titov, 2001; no event page at http://nctr.pmel.noaa.gov/database_devel.html).

A truncated post-earthquake and tsunami survey by helicopter took place on 9 December 1997 (Leonov, 1998; Zayakin and Pinegina, 1998). The survey reached as far north as Kronotsky Cape on the Kronotsky Peninsula (Fig. 1) and found that the tsunami had not exceeded the unvegetated beach. At this time, the beach was covered with a thin layer of ice and snow, which in places had been coated by the tsunami with a thin sand layer and elsewhere had been broken up by the tsunami (Fig. 3). The team did not have surveying equipment and estimated runup to be no more than 3 m (T. Pinegina notes), and the published report gave a maximum of 1-1.5 m. The turnaround point in the survey was dictated by fuel and available daylight.

On 5 December 1997, two rangers were in a cabin near Big Chazhma River; one of them was interviewed (in Petropavlovsk-Kamchatsky) by T. Pinegina 19 April 2001. They felt the earthquake that night, and the next day, as was their custom, they went via snowmobile to survey the northern coastal part of Kronotsky reserve, to the Little Chazhma River area. At the mouth of the Big Chazhma, they saw jumbled ice and seaweed on the snow; a cabin on

149 the south bank of the Little Chazhma River was partly wetted, and there was seaweed on the snow. Normally the

150 rangers crossed the river near this cabin, but the river was a jumble of ice and they had to go some distance upstream

151 in order to cross (on ice). On the other side, they could not continue north because there was water in the low spot

152 between beach and hill (see Fig. 4, our profile 100).

153   Based on results of the post-tsunami survey (reported to Sohn by V. Gusiakov), Sohn (1998) analyzed the

154 tsunami with regard to its earthquake source and concluded that the main rupture must have lain largely under land,

155 in order to explain the low runup accompanying a moment magnitude she calculated as Mw 7.7. However, the

156 tsunami amplitudes on tide gages in Hawaii indicate that there was substantial subsea deformation.

157

159 **Figure 3.** Photos taken by T. Pinegina on 9
161 Dec 1997 near Kronotsky Cape (location on
163 Fig. 1). For additional photo and sketch for
165 context, see Fig. S3. **Above**: the tsunami
167 deposited sand on above the snow up to about
169 the line of grassy vegetation at the back of the
171 beach (helicopter for scale). **Lower left**: Ice
173 and snow broken up by the tsunami (excerpted
175 from photo in Fig. S3). **Lower right**: detail of
177 tsunami-deposited sand above snow that
179 covered the beach. Compass for scale.

181
183
185
187
189
191
193
195
197
199
200

201 **2.3 Historical record of earthquakes and tsunamis affecting the field area**

202   The Kamchatka Peninsula has a short but rich historic record of large earthquakes and attendant tsunamis,

203 of which we discuss herein only 20th century tsunamis originating in or having been recorded in the field region of

204 southern Kamchatsky Bay (Table 1). In addition to locally originating tsunamis, Kamchatka is vulnerable to

205 tsunamis originating from Chile, less so from Peru, and not so much from Japan, Alaska, Aleutians and Central

206 America, due to directivity (e.g., see Table S1). Based on existing scant records in the vicinity of the field area

207 (Table 1), we can expect the 1960 Chile tsunami to have reached elevations of 3-5 m above sea level in the field area,

208 on the order of twice as high as the 1952 southern Kamchatka tsunami *at these same localities*.

Table 1. 20th CENTURY TSUNAMIS AFFECTING THE KAMCHATSKIY BAY COAST OF KAMCHATKA*

EARTHQUAKE PARAMETERS			RECORDS OF TSUNAMI RUNUP (*tide gage records in italics*) in meters									MAX KAM	Hilo, HI
			Locations South to North (see Figure 1)										
Date (local)	Source region	Mw	Kron Bay	Kron. Cape	**Chazhma - Adr-Bistr R.**	Shuber- tovo	1st River s. of U-K	Tsutsumi s. of U-K	*U-K tide gage*	Dembi Spit, U-K	Bering I. (south)		
5-Dec-97	**Kronotskiy Peninsula**	7.8/7.9^	0.5-1	1.5	this paper				*gage broken*		*incompl record*	**this paper**	*0.24*
15-Dec-71	Commander Is.	7.8^							*0.47*				*0.10*
23-Nov-69	Bering Sea	7.7							*0.2*			10-15	*0.10*
24-May-60	**Chile**	9.5	4				3		*0.8*	3-4	3-3.5	7	*~10*
05-Nov-52	**s. Kamchatka**	9	10-13			0.5-1			*0.1*		2	10-15	*1.1*
14-Apr-23	**Kamchatskiy Bay**	7.3/8.2^					20#	>5		11#	4	20	*0.30*
04-Feb-23	**Kronotskiy Bay**	8.5^	6-8		4-5 km up Chazhma			~4				6-8	6.10

*Bold: tsunamis most likely to leave a sedimentary record in south Kamchatsky Bay; see Supplemental Table 1 for a more complete list of tsunamis and Supplemental Table 4 for specifics in 1923 cases. Primary sources: Zayakin and Luchinina, 1987; NCEI (formerly NGDC) Natural Hazards Data, online (see references)

^Kamchatka Mw's from Gusev and Shumilina, 2004; G&S 8.2 for 14Apr23 is based on tsunami; see text discussion

#The 20-m and 11-m numbers are from higher-relief shorelines than the other measurements

209
210

211   The largest documented local tsunamis from earthquakes near Kronotsky Peninsula (Fig. 1; Table 1) are
212 two from 1923, both having local as well as farfield records (Table S4); both may have been large in south
213 Kamchatsky Bay. There was also a 24 Feb 1923 Mw 7.6 earthquake in this area (Fig. 1; Gusev, 2004); however, it
214 has no historical tsunami record in the near or far field. [The Mw 8.0 1917 earthquake along the Bering fracture
215 zone (Fig. S1) also did not produce an observed tsunami.] The 3 Feb 1923 Kronotsky Bay earthquake (Mw 8.5) was
216 located south of Kronotsky Cape (Fig. 1). The 14 April 1923 north Kamchatsky Bay earthquake (Mw 7.3 in NCEI
217 catalogue) generated a high tsunami near Ust-Kamchatsk (Table 1; Table S1). Based on tsunami amplitudes, Gusev
218 and Shumilina (2004) suggested this April 1923 earthquake had a moment magnitude of 8.2 (Table S1, Fig. S2).
219 Based on the estimated locations of the February and April sources (Fig. 1) and the recorded tsunami runup in Ust-
220 Kamchatsk (Table 1), we might reason that in south Kamchatsky Bay the April 1923 tsunami may have been larger.
221 However, Zayakin and Luchinina's catalogue records that the February 1923 tsunami went 4-5 km up the Chazhma
222 River (Table 1).

223   The record of earthquakes and tsunamis on Kamchatka prior to the 20th century is spotty but improving
224 (Zayakin and Luchinina, 1987; Godzikovskaya, 2010); the earthquake catalogue from the second half of the 19th
225 century is not as complete as from before or after (Gusev and Shumlina, 2004).
226 Earthquakes on 17 May 1841 and 17 October 1737 originated in the region of the 1952 south Kamchatka great
227 earthquake, so likely did not have significant effect in southern Kamchatsky Bay (see Table 1, 1952 runup). Other
228 tsunamis that may have affected south Kamchatsky Bay are an autumn 1849 tsunamigenic earthquake in the vicinity
229 of the Komandorsky Islands (Godzikovskaya, 2010) and a 1791 event which has an intriguing account of having
230 affected the mouth of the Kamchatka River (Ust-Kamchatsk), reaching 7 km upstream (Zayakina and Luchinina,
231 1987).

3 Methods

We measured 15 topographic profiles (Fig. 4) perpendicular to the shoreline along the coast of southern
Kamchatsky Bay (Fig. 1), and made 117 excavations along these profiles in order to document historical and
paleotsunami deposits. We used a surveying rod with a transit level (hand level and tape for profile 001 and upper
part of profile 120) (methods as in Bourgeois et al., 2006).
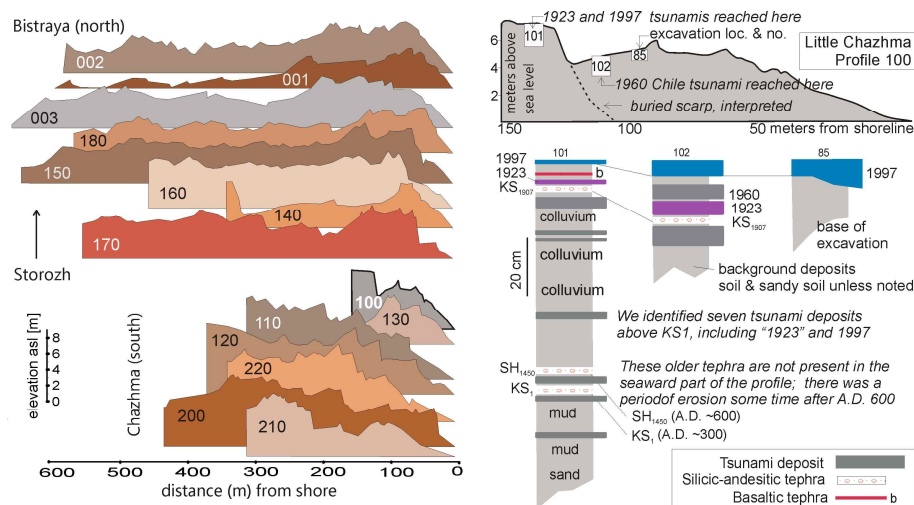
Figure 4. Left. Topographic profiles measured in southern Kamchatskiy Bay (locations on Fig. 1, arranged from
south (bottom) to north (top), except 001 and 002 reversed to reveal topography. Distances and elevations are
measured from 0 at the water line, corrected to low tide. **Right**: Chazhma Profile 100 used as a key to collected
profile data and interpretations *(interpretation in italics)*; background deposits are soil or sandy soil, unless noted.

Tsunamis create sedimentary deposits as they flood the coast with turbulent, turbid water. The general
characterization of a tsunami deposit in sandy coastal systems is a sand sheet that typically thins and fines landward,
following topography (Bourgeois, 2009). Many factors, from sediment availability to coastal topography and
roughness to the velocity profile of incoming and outgoing waves, play a role in sedimentation. Kamchatka field
sites are primarily sandy, vegetated coastal plains and associated peat marshes, where availability of sand and the
vegetative cover maximize the likelihood of generating and preserving tsunami deposits. (Many historical
Kamchatka tsunamis have occurred during winter snow cover; deposits would have been "let down" onto a
vegetative mat as the snow melted.) The maximum distance inland of a tsunami deposit (*sediment inundation*, Fig.
5) and the deposit's elevation at sediment inundation (*sediment runup*, Fig. 5) represent minimum estimates of
tsunami extent for several reasons. Tsunami deposits can only be more limited (not more extensive) than water
runup and inundation, the final limit of a deposit is not always located in the field, and thin deposits may not be
identified or preserved.
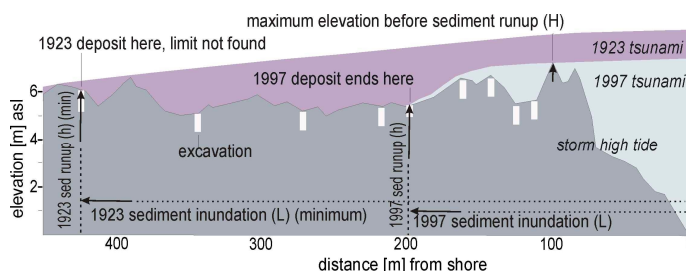
Figure 5. Terminology for sediment runup and sediment inundation, and interpretation of deposits from 1997 and 1923, using example of an actual profile (Storozh 160; vertical exaggeration ~10). Note that near the shoreline, both tsunamis had to exceed a point (H) higher than "sediment runup" (h) and that, although the minimum sediment runup for 1923 is not much greater than for 1997, 1923 had to have been higher to generate greater inundation. Distances and elevations are from surveying.

Primary age control in excavations is provided by dated regional and local marker tephra layers (Table 2), which in general have been well studied on Kamchatka (e.g., Braitseva et al., 1997), although tephra in the south Kamchatsky Bay area had not previously been examined. Based on our own and previous work, as well as on more recently published isopach maps (Kyle et al., 2011; Ponomareva et al., 2017), the three most consistently present layers in the sections are $KSht_3$ (A.D. 1907 — we label KS_{1907} on diagrams)—most useful for studying the historical record, SH_{1450} (A.D. ~600) and KS_1 (A.D. ~300), the latter used as the lower boundary for our tsunami statistics. In more northern profiles, SH_2 (A.D. ~1130) is commonly present. Recent work around Shiveluch volcano and Kamchatsky Peninsula (Fig. 1) has led to redesignation of Shiveluch tephras and to more definitive model ages of these tephra (Ponomareva et al., 2017). In addition to the silicic marker tephra (Table 2), there are local basaltic-andesitic tephra layers, which can be from Kliuchevskoi, Bezymianny, Tolbachik or Gamchen volcanoes; we used these tephra only as local field guides. In the northernmost of our profiles, a historic ash from Bezymianniy 1955 (year before the 1956 paroxysmal eruption) is locally present and a factor in distinguishing the Kamchatka 1952 from the Chile 1960 tsunami deposits.

Table 2. Marker tephra layers younger than 2000 years old in shoreline profile sections, southern Kamchatsky Bay*

Code Field/Classic^	Code New*	Source volcano	Modeled age* (years B.P.)	Assigned age* (calendar years)	Field description	Field thickness
$KSht_3$	$KSht_3$	Ksudach	Historical	A.D. 1907	Light to medium gray, fine to very fine sand	0.5-2 cm
SH_2	SH#6	Shiveluch	817 +59/-57	A.D. 1134	White (faint gray, yellow white), fs-vfs, has pumice	0.5-1 cm; distinct toward north
SH_{1450}	SH#12	Shiveluch	1356 +52/-45	A.D. 596	Pale yellow, yellow gray, lt gray, vfs-ms, salt & pepper —grainy	1-2.5 cm; typically 1-2 cm
KS_1	KS_1	Ksudach	1651 +54/-61	A.D. 298	Lt brown, beige, "coffee cream"; thin gray cap; si-vfs	1-3 cm; usually not >2 cm

*Ponomareva et al., 2017

^Braitseva et al., 1997

278   For the prehistoric record of tsunami runup and inundation, topographic profiles would not necessarily be

279   the same as in the recent past must be reconstructed to account for succeeding topographic changes in elevation and

280   distance along the profile. While we cannot typically reconstruct profiles that have been changed by erosion, we can

281   reconstruct profile progradation (building seaward), which affects profile width. Our method uses preserved tephra

282   as discussed, e.g., in Pinegina et al. (2013) and MacInnes et al. (2016). Changes in elevation are quantified by

283   determining the age and elevation of the lowest former soil horizon above marine sand in any excavation (as in

284   Pinegina et al., 2013).

285

286   **3.1 Field localities**

287   The southern field site (Fig. 1), which we call "Chazhma," is a narrow strip (~400 m wide or less) of

288   Holocene accumulative coastline along a rugged coast just north of the Kronotsky Peninsula. The two profiles near

289   river mouths (Chazhma 210 and Chazhma 130; Fig. 4) maintain lower elevations (< 4 m) over much of their

290   distance, though both reach elevations of more than 6 m above sea level. The other five profiles rise, typically in

291   sharp steps indicative of Holocene uplift events (e.g., Pinegina et al., 2013), reaching typical maximum levels of 8-

292   10 m (Fig. 4). Net uplift on these profiles is consistent with longer-term uplift of Pleistocene terraces on the

293   Kronotsky Peninsula (Melekestsev et al., 1974).

294   The northern field site, which we call "Storozh," extending north to the Bistraya River (Fig. 1), is a broader

295   strip (typically 600 m wide) of Holocene accumulative coastal plain associated with active and drowned river

296   mouths. Two of these profiles (140, 001) drop in elevation behind one or more beach ridges (Fig. 4). The other

297   seven profiles are typified by a series of beach ridges, of which the seaward ridges are higher, reaching typically 6-7

298   m, with an average elevation of the profile in the range of 4-6 m (Fig. 4). Such profiles indicate mild subsidence or

299   no vertical change in the late Holocene.

300

301   **4 Results -- 20th century tsunami deposits**

302   In field season A.D. 2000, the sand we interpret to have been deposited by the 1997 Kronotsky tsunami

303   formed a sheet-like layer at the surface, buried only by grass, leaves and other dead vegetation. The deposit we

304   interpret to be "1923" (from one or both of two tsunamis in 1923) lies above the marker tephra KS_{1907} with less soil

305   thickness between KS_{1907} and "1923" than between the top of "1923" and the base of the modern turf. Our

306   interpretation of "1923" as well as a rare sand layer between "1923" and 1997, which we assign to the 1960 Chile

307   tsunami, is discussed below.

308   Using identified and mapped tsunami deposits, we calculate minimum sediment runup and inundation on

309   each of the 15 profiles (Table 3, Figure 6), correcting for tide at the time of survey. We determine minimum

310   sediment runup (h) by the presence or absence of distinct 1997 and "1923" deposits on each profile. We distinguish

311   between profiles where the farthest landward excavation still contains the 1997 or "1923" deposit and ones that do

312   not. If no deposit is present in one or more excavations landward of ones with a deposit, the limit of sediment

313   inundation (L) occurs within the measured profile (Fig. 5, example of 1997) and actual tsunami runup is estimated

314   from sediment runup. For profiles where a particular tsunami deposit extends beyond all excavations (Fig. 5,

315 example of 1923), the actual size of the tsunami could be, in some cases, significantly greater than our sediment-
316 runup and inundation minima. We also report the maximum height the tsunami had to exceed (H) as it traveled
317 along (across) a profile. Note that maximum elevations and inundation distances are affected by elevations and
318 distances along actual profiles (Fig. 4). In a few cases, the farthest inland excavation was at a low elevation that
319 could have been reached via the river rather than over the profile (Table 3, Fig. 6).
320

321 **4.1 1997 tsunami**
322 Sediment runup data (Table 3, Fig. 6) indicate that north of the Kronotsky Peninsula the 1997 Kronotsky tsunami
323 ran up to as much as 9.5 m, averaging 6.1 m, with moderate inundation distances of 100-300 m. The general pattern
324 over about 100 km of coastline, including post-tsunami survey observations on Kronotsky Peninsula itself, is
325 relatively smooth. The maximum elevation reached by the tsunami deposit is higher on southern (Chazhma) profiles.
326 However, lower runup numbers on northern profiles may be an artifact of their lower elevations (Figure 4);
327 inundation distances are greater on these profiles (Table 3). On some profiles the 1997 deposit is absent.
328

329 **4.2 1923 tsunamis**
330 Sediment runup and inundation data for "1923" indicate that this tsunami was larger than 1997. The deposit we
331 interpret as from 1923 is usually thicker and more extensive, and never less extensive, than the deposit from 1997.
332 The "1923" deposit is present on all measured profiles whereas the 1997 deposit is missing on six (Table 3, Fig. 6).
333 Only on profiles where the sediment limit was not found (e.g. 100), or where profiles dropped to low elevations at
334 their landward extent (001, 180, 160, 140, 100, 130, 210) were "1923" deposits at similar or lower elevations than
335 1997, and in many of these cases (001, 180, 160, 130), inundation distances for "1923" were longer. Even in the
336 few cases where our field observations did not distinguish the two by sediment runup or inundation, the "1923"
337 deposit was coarser and/or thicker than 1997.
338

339 **Figure 6.** Water (Zayakin and Pinegina, 1998) and
340 sediment runup (this paper, Table 3) for the 1997
341 Kronotsky tsunami on and north of the Kronotsky
342 Peninsula, southern Kamchatsky Bay (locations on Figure
343 1). Water runup was not measured with instruments but
344 estimated; tsunami did not exceed the unvegetated beach
345 (e.g., Fig. 3); it could have been somewhat higher than
346 reported, shown by dashed blue line. Sediment runup is
347 also illustrated for the tsunami deposit closely above KS_{1907},
348 which we interpret as from 1923 February or April (see
349 text discussion). Sediment inundation is given in Table 3,
350 as well as latitudes and longitudes for the 15 profiles.
351 Figures 4 and 5 illustrate methods and terminology.
352
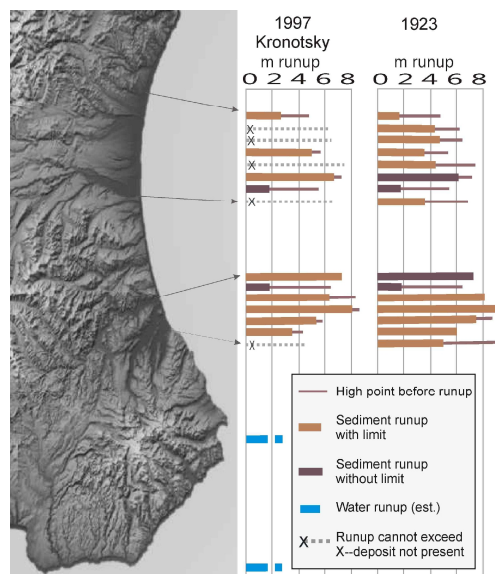
Table 3. Sediment runup and inundation for historical tsunamis above KS_{1907}, southern Kamchatsky Bay

Region	Profile #	Latitude	Longitude	1997			1960			1923		
				h	L	H	h	L	H	h	L	H
Bistraya River	001	55.6226	161.7799	3.4	200	5.3	3.3	**126**	5.3	2.0	250	5.3
	001 via river									0	**650**	*
Bistraya River	002	55.59735	161.76802							4.4	205	6.2
	002 via river									2.2	560	*
Bistraya River	003	55.57814	161.76001							4.8	211	6.5
Adrianovka R.	180	55.52745	161.74836	4.8	118	5.6				3.5	367	5.6
Storozh River	150	55.48508	161.74135							2	645	7.7
Storozh River	160	55.45819	161.73936	6.6	159	7.5	**6.2**	107	7.5	6.1	419	7.5
Storozh River	140	55.4387	161.7393	5.8	**330**	5.8				5.8	330	5.8
Storozh River	170	55.38604	161.73401							3.6	267	6.7
Little Chazhma R.	100	55.1407	161.8281	7.4	125	7.4	4.5	107	6.2	7.4	125	7.4
Little Chazhma R.	130	55.1235	161.8379	4.4	109	6.3	4.4	78	5.1	1.8	158	6.3
Chazhma	110	55.1181	161.8408	6.6	200	8.3				8.1	315	8.3
Chazhma	120	55.1019	161.8514	**9.5**	200	9.5				**12**	380	9.5
Big Chazhma R.	220	55.0794	161.8679							7.7	335	9.8
Big Chazhma R.	210	55.071	161.876	6.0	305	8.0				6	305	8
Big Chazhma R.	200	55.0629	161.8879							6.6	361	9.1
	200 via river									5	428	*
			AVERAGES	*6.1*	*194*	*7.1*	*4.6*	*105*	*6.0*	*4.9*	*346*	*7.3*

h - elevation of excavation m a.s.l.; equals "sediment runup" (maxima in bold)

L - distance from the shoreline, m; equals "sediment inundation" (maxima in bold)

H - highest elevation, m a.s.l., between shoreline and excavation; must be exceeded where there is a deposit (max. in bold)

353   *If* the tsunami reached a low inland point via the river (indeterminate), H from the profile is not relevant.

354

4.3 Chile1960 deposit

356   Between "1923" and 1997 deposits on a few profiles (Table 3), there is a thin, patchy and less extensive deposit

357   which we attribute to the 1960 Chile tsunami (e.g., Fig. 4, right). We favor 1960 over 1952 Kamchatka because the

358   1960 tsunami was larger than 1952 in the Kamchatsky Bay region (Table 1). Also, The more locally generated 1952

359   tsunami dies off in amplitude along strike of the rupture (MacInnes et al., 2010), whereas the Chilean tsunami on

360   Kamchatka is little affected by latitude (Zayakin and Luchinina, 1987). Supporting the 1960 interpretation, in one

361   excavation on profile 001, this intermediate tsunami deposit lies above the Bezymianny 1955 tephra layer.

362

4.4 Historical tsunami deposit close below KS_{1907}

364   In many excavations (e.g., Fig. 7), there is a tsunami deposit within a few cm of the base of $KSht_3$ and which is

365   comparable to 1997 and 1923 in thickness and extent. Although pre-1907 sedimentation rates are difficult to

366   determine this tsunami deposit must fall within the historical period, which extends back to 1737. However, the

367   more complete historical records are from southern Kamchatka, and the second half of the 19th century record is

368   particularly spotty (Gusev and Shumulina, 2004). Thus we cannot assign a specific event to this deposit.

369

5 Discussion – 1997 and "1923" Deposits

5.1 1997 tsunami

Our observations are consistent with 1997 being a seismogenic tsunami source with significant rupture energy expended in the northern portion of the zone of aftershocks. The extensive and relatively smooth distribution of runup (Table 3; Fig. 6) and the ratio of maximum runup to distance over which the tsunami had significant runup (on the order of 10^{-5}) indicate that this tsunami was typical of a seismogenic source rather than a landslide source (cf. Okal and Synolakis, 2004). The far-field tide-gage records (e.g., Hilo, Table 1) are also indicative of a broad rather than a point source. Given that the post-tsunami survey reported runup that did not exceed the beach on the Kronotsky Peninsula and that the deposits we mapped north of the peninsula are from the 1997 tsunami, *any source model must explain low runup on the peninsula and relatively high runup north of the peninsula*. Source region models by Bürgmann et al. (2001) and Llenos and McGuire (2007), e.g., do not include the northern aftershock area, and such models have been used to interpret Kamchatka subduction-zone behavior (e.g., Song and Simons, 2003; Bürgmann et al., 2005; Llenos and McGuire, 2007; Bassett and Watts, 2015). On the other hand, source regions by Gusev et al. (1998; also Gusev, 2004) and Levina et al. (2013) tend to include the entire aftershock zone, overlapping Feb 1923 in the south but also filling the gap between Feb 1923 and April 1923 (Fig. S1). Zobin and Levina (2001) favor most mainshock energy being generated in the middle zone defined by fewer aftershocks (see Fig. 2); Slavina et al. (2007) interpret the southwestern aftershock activity (Fig. 2) to be on a separate, transverse fault; Kuzin et al. (2007) also interpret the SW portion of the (extended) aftershock region to be a separate stress zone. A recently published finite fault model resolves to most deformation being under the Kronotsky Peninsula, with most energy release focused in the north (Hayes, 2017; https://earthquake.usgs.gov/earthquakes/eventpage/usp0008btk#finite-fault).

5.2 1923 tsunamis

There are reasons to favor either or both the 3 February 1923 and the 13 April 1923 Kamchatka tsunamis as the generator(s) of the deposit above KS_{1907} that we identify as "1923." Given what is known, south Kamchatsky Bay is the place most likely to have *comparable* runups from each. Both tsunamis have a record in Hilo, but one is runup and the other tide-gage amplitude (Table 1). There is no case on Kamchatka of a pair of similarly measured records from the same locality with which to compare the two tsunamis, with the exception of observations that the April tsunami generated more damage at the Tsutsumi fish plant southeast of Ust-Kamchatsk (Table S4). The 3 February tsunami was larger in most catalogued locations (Table S4) but apparently smaller than April 1923 in *north Kamchatsky Bay*. The two 1923 tsunamis both occurred while the ground would have been snow covered so that following snowmelt, it would be nearly impossible to distinguish two different deposits in this case. The source regions of the two 1923 Kamchatka tsunamis have been mapped (Fig. 1) but are not easy to constrain in detail other than that the February earthquake was south of Kronotsky and the April earthquake north of it. The February earthquake has been catalogued as Mw 8.3 and the April earthquake as Mw 7.3 (Table S3), but the local and far-field tsunami runup for April 1923 suggests it was significantly larger (Gusev and Shumilina, 2004); Gusev suggests

406   Mw 8.2 for the April earthquake. A moment magnitude around 8 would be more consistent with its tide-gage
407   amplitude in Hilo (Fig. S2).
408

5.3 Chile1960 deposit

410   Between "1923" and 1997 deposits on a few profiles (Table 3), there is a thin, patchy and less extensive deposit
411   which we attribute to the 1960 Chile tsunami (e.g., Fig. 4, right). We favor 1960 over 1952 Kamchatka because the
412   1960 tsunami was larger than 1952 in the Kamchatsky Bay region (Table 1). Also, the regionally generated 1952
413   tsunami decreases in amplitude toward the north on Kamchatka (Zayakin and Luchinina, 1987; also see MacInnes et
414   al., 2010), whereas the distally generated Chilean tsunami on Kamchatka is little affected by latitude. Supporting
415   the 1960 interpretation, in one excavation on profile 001, this intermediate tsunami deposit lies above a Bezymianny
416   1955 tephra layer (Fig. 7).
417

5.4 Historical tsunami deposit close below KS$_{1907}$

419   In many excavations (e.g., profile 100 in Fig. 4, Profile 110 in Fig. 8), there is a tsunami deposit within a few cm of
420   the base of KS$_{1907}$ and which is comparable to 1997 and 1923 in thickness and extent. Although pre-1907
421   sedimentation rates are difficult to quantify this tsunami deposit must fall within the historical period, which extends
422   back to 1737. However, we cannot assign a specific event to this deposit; the more complete historical records are
423   from southern Kamchatka, and the second half of the 19th century record is particularly spotty (Gusev and
424   Shumulina, 2004).

Figure 7. Northernmost profile, southern Kamchatsky Bay (Fig. 1 location; more extensive key in Fig. 4). This
profile shows evidence of subsidence through time -- the landward part of the profile is lower. This lower profile
has been subjected to river erosion -- the "mixed zone" is mostly fluvial sediment containing clasts of older material.
Excavations having this mixed zone (273 to 270) all contain a tephra older than KS$_1$, indicating that older strata are
preserved below the reworked material. In this profile 001, there is an ash layer from the 1955 eruption of
Bezymianny, a year before its major eruption. With this tephra present, we can assign the tsunami deposit above (in
excavation 267) to Chile 1960 rather than to Kamchatka 1952.

Figure 8. Profile 110, Chazhma area (Fig. 1 location; more extensive key in Fig. 4). This profile has been uplifted through time – the landward part of the profile is higher. Exc. 45 contains many tsunami sand layers currently at high elevation, which when reconstructed were lower (Fig. S5). The profile shows the distribution of 20th century deposits, as well as a tsunami deposit very close below KS_{1907}. The 1923 tsunami(s) reached the highest point shown on this profile, whereas 1997 and "below KS_{1907}" were smaller. The deposit we tentatively assigned to Chile 1960 on this profile is not included in Table 3 because the deposit was not well preserved; it is higher than any other excavation containing a deposit we attribute to Chile 1960.

6 Tsunami deposits pre-20th century back to KS_1 (~A.D. 300)

Goals in reconstructing paleotsunami history include both scientific and practical objectives. Scientifically, southern Kamchatsky Bay paleotsunamis can help us see patterns of subduction zone behavior. Are the historical tsunamis (and their generating earthquakes) comparable to events in the past? What is the "typical" event and what are the rupture patterns of the northern Kamchatka subduction zone? Practically, these questions apply also to probabilistic hazard analysis – at what frequencies do tsunamis occur and what is their size-frequency relationship?

6.1 Occurrence and Size

For the record and analysis of tsunami deposits below KS_{1907}, for each excavation we count the number of deposits between marker tephra and determine the approximate elevation above sea level and distance from shore of the excavation locale in that time (tephra) interval (Fig. S5). For some deposits, this excavation may be their limit and for others not (e.g., Fig. 9). We do not attempt to correlate sand layers from excavation to excavation (or profile to profile), though there are cases where it is possible. Rather, we count the maximum number of tsunami deposits between tephra, which is our indication of how many tsunami events have occurred.

459
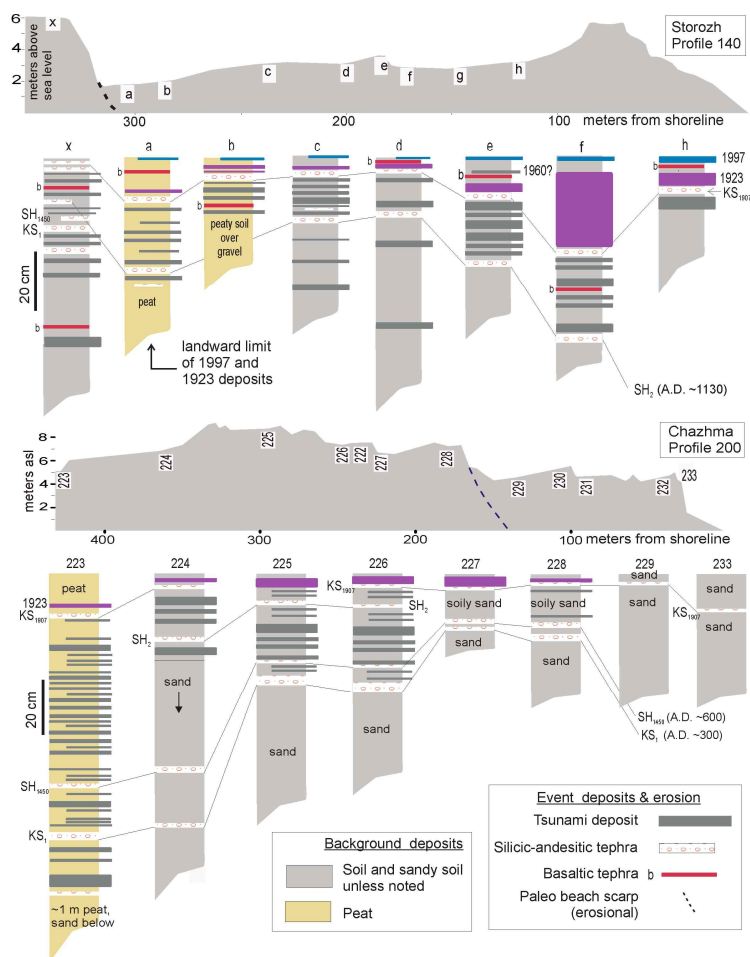
Figure 9. Example of two profiles that illustrate paleotsunami deposits used in analyses. Also see Figs. 4, 7, 8)
Storozh Profile 140 (top). Here we use this profile to illustrate an analysis of tsunami deposits between KS_{1907} and
SH_2; note that the deposits thin landward, in general. In most excavations there are six tsunami deposits between
KS_{1907} and SH_2; excavation "x" has only three. Thus all six tsunamis reached "a" but only three reached "x"; or,
three of the six tsunamis only reached "a". All six tsunamis had to exceed the height of the shoreward beach ridge.
Chazhma Profile 200 (bottom). As in Profile 110 (Fig. 8) this profile has undergone uplift through time. For sub-
SH_2 deposits, the profile was reconstructed to 4 m lower and 150 m narrower. Sites 229-233 are young; the profile
from 228 landward is older than KS_1 (A.D. ~300). Site 223 is not far from the modern Chazhma River and in the
past some tsunamis may have flooded this site via the river, when the profile was lower. Sites 226 and 225 both
have six deposits between SH_2 and SH_{1450}; no other excavation on this profile provides a good count in this interval,
but these six deposits probably are in the record at 223, and 224 was simply too sandy to count all layers in this
interval. SH_2 is not preserved (was not detected) in the peat excavation (223), but the 23 tsunami deposits in this
excavation can be used in the overall count above KS_1. Excavations 223, 225 and 226 all preserve tsunami deposits
between SH_{1450} and KS_1. In this interval the peat excavation (223) contains six deposits to the two in 225 and 226,
for two possible reasons; first, peat is a better preserver/displayer of thin layers, and second, 223 is lower than 225
and 226 and at this time all were closer to shore. For the latter reason, 223 may have received tsunamis and their
deposits directly from the river rather than over the beach ridge(s).

477   In order to summarize paleotsunami sizes, we determine sediment runup--or the highest point seaward,

478 whichever is higher--and sediment inundation for tsunami deposits on each profile. For each tephra interval along

479 each profile, there will be deposits at maximum distances and maximum elevations; the two measures are treated

480 separately because tsunami deposits are not correlated (in fact, high runup is associated with shorter, steeper profiles

481 and long inundation with low-relief profiles). For example, for the historical deposits, two points are plotted (Fig.

482 10) – their point of maximum inundation and their point of maximum runup, which are on usually on separate

483 profiles.

484   A few of the paleo-events are comparable to Chile 1960 (Fig. 10), but most are likely from locally

485 generated tsunamis because Chile 1960 was an outsized event and its deposits is not well represented on the profiles.

486 The 1997 tsunami has dimensions similar to the majority of paleotsunamis as represented by sediment runup of on

487 the order of 5-7 m (Fig. 10). The "1923" deposit, for which we do not know if related to February or April or both,

488 is a "typical largest" event (Fig. 10). Recall that in these field sites there are few excavations at elevations of 10 m

489 or more (Fig. S6), and that these higher elevations are on uplifted profiles, so we do not have a record of older

490 paleotsunamis reaching such elevations, simply as an artefact of the data and analysis (Fig. S5). This issue is

491 present also for paleo- inundation on prograding profiles, but is not such a strong artefact in this dataset. Overall,

492 the number of deposits tends to decrease away from the coast and at higher elevations (density of points on Fig. 10),

493 although there is a lot of scatter in the data, likely due to preservation and identification differences (e.g., Fig. 9).

494

495 **Figure 10.** Three-dimensional diagram summarizing
496 sediment runup and inundation for tsunami deposits,
497 south Kamchatsky Bay, above KS_1 tephra (A.D. ~300, up
498 through A.D. 2000) (from data plotted in Figs. S7 and S8).
499 The three historical tsunami deposits are highlighted with
500 their two points of maximum runup and maximum
501 inundation, which do not coincide. For prehistoric events,
502 we calculated (sediment) runup and inundation per tephra
503 interval, with adjustments for changes through time in
504 shoreline location and excavation elevation (see text and
505 Fig. S5). The axis "average time between deposits" is
506 biased by deposit counts and short time intervals but is
507 shown here for general pattern.

508

509

510 **6.2 Recurrence**

511   To determine tsunami recurrence according to size, we consider all tsunami deposits above KS_1 (A.D.

512 ~300) (Fig. 11). There are intermediate Shiveluch tephra layers between KS_{1907} and KS_1 (Table 2), but their

513 presence is not consistent enough to break down recurrence statistics, and the time intervals are relatively short

514 relative to the number of events, so statistical analysis cannot be supported. For this exercise, we only use

515 excavations now at or reconstructed to be more than 5 m above sea level or landward of a beach ridge (reconstructed

516 to be) higher than 5 m. The grand total of the maximum number of events per each interval is 18 deposits, including
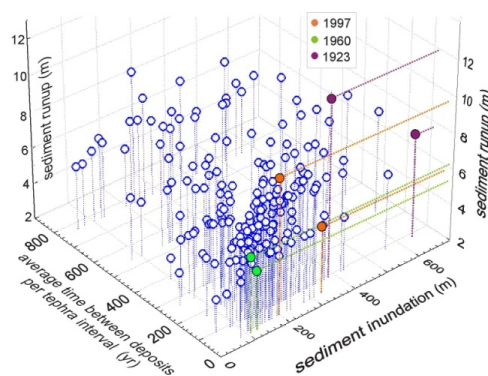
517   the historical cases. For each event, we determine a maximum sediment runup, that is, if there are four deposits

518   between two marker tephra on a given profile, we determine the four highest points those deposits reach; e.g., two

519   may reach 8.3 m and the other two only 7.2 m (all four reaching 7.2 m). We use reconstructed distances and

520   elevations for each time interval below KS_{1907}. The maximum elevation is either sediment runup, h, or maximum

521   elevation before sediment runup, H (as in Fig. 5), whichever is higher. Independent of the determined maximum

522   elevation, we determine a maximum sediment inundation for each deposit in each tephra interval.

523   All 18 deposits reached elevations of 5 m (smaller not considered) and inland distances of 100 m, each

524   factor with a recurrence interval of about 100 years (Fig. 11). Note again that runup and inundation are not paired;

525   high runup commonly occurs on shorter, steeper profiles and long inundation on lower profiles. Tsunamis reaching

526   an elevation of at least 7 m have a recurrence of ~200 years (Fig. 11). The largest reconstructed tsunamis as

527   recorded by tsunami deposits have runup of 10 m or more and occur on average every 425 yr. Tsunamis with

528   inundation of 600 m or more occur on average every ~570 yr.

529

530   **Figure 11.** Tsunami (>5 m) recurrence for
531   exceeded elevations (sediment runup) and
532   exceeded distances from shoreline (sediment
533   inundation) of tsunami deposits since KS_1 (A.D.
534   ~300) in south Kamchatsky Bay. (For runup,
535   integers of m are shown; for inundation,
536   multiples of 100 m.) For example, tsunamis
537   with runup of 8-9 m or more occur on average
538   every 283 years. Tsunamis exceeding
539   inundation of 500 m occur on average every
540   340 years. Recall that runup and inundation are
541   not paired (see text).

542

543

544   **7 Discussion and conclusions**

545   **7.1 Historical tsunamis**

546   This work adds to the tsunami catalogue for 1997 Kronotsky and 1960 Chile, but not February or April

547   1923 Kamchatka events because we cannot differentiate the (two) 1923 deposits. The nearfield nature of the 1997

548   Kronotsky tsunami is significantly revised by this study of coastal profiles north of the Kronotsky Peninsula, adding

549   substantial data to its catalogue. The 1997 tsunami reached runup heights of more than 9 m, averaging 6 m over

550   about 60 km of coastline. As would be expected, tsunami heights (as indicated by deposits) and inundation

551   distances are influenced by the coastal topography, with higher runups on steep profiles and higher inundation on

552   lower-relief profiles. Data catalogues do not commonly provide topographic profiles, yet this information can be

553   critical to understanding a tsunami and its generating source.

554   Based on deposits from 15 profiles and more than one hundred excavations, we conclude that the 1923

555   tsunami (February or April indeterminate) was larger than the December 1997 Kronotsky tsunami, but the summary

556   and tabulated data (Fig. 6, Table 3) are tricky to interpret, with sediment inundation (L) being more indicative of
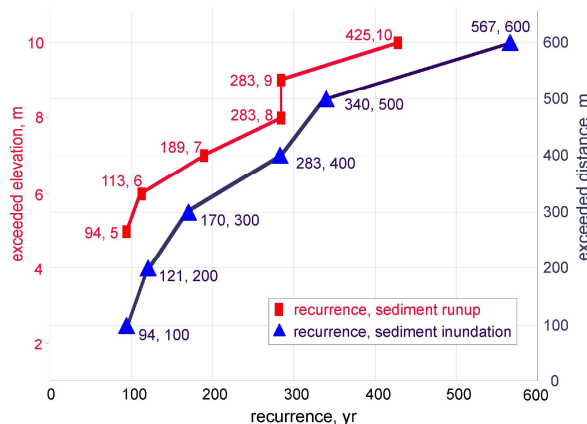
557 tsunami size than runup (h) or highest point seaward of runup (H). On the basis of the total number of profiles

558 exhibiting a deposit, "1923" is more extensive, but its average sediment runup (h) value is lower because the farthest

559 point it reached on a number of profiles is actually lower than the points for 1997. Moreover, even though "1923"

560 exceeded more of the high beach ridges seaward of the (sediment) runup point (H), the average of those is almost

561 the same as for 1997 (Table 3). The most telling measurements distinguishing 1997 from "1923" are sediment

562 inundation distances, with the average for "1923" almost twice that for 1997.

563   The 1952 tsunami deposit in southern Kamchatka (and the northern Kuril Islands) (MacInnes et al., 2010)

564 reaches greater heights and inundation distances along its earthquake rupture zone than any of the historical tsunami

565 deposits along the northern part of the Kamchatka subduction zone (this study; Pinegina, 2014). While this

566 observation is not surprising given that 1952 was Mw 9.0 and the historical events to the north no larger than about

567 Mw 8.5, the question to address is, can (does) the northern part of the subduction zone produce Mw 9 events, or

568 does Kronotsky Cape represent an asperity that keeps ruptures shorter, as in 1923? For that, we must turn to the

569 prehistoric record.

570

571 **7.2 Implications for the 1997 Kronotsky earthquake rupture and the 1923 events**

572   The sediment runup and inundation data reported here require a reevaluation of rupture source models for

573 the 1997 Kronotsky earthquake; models which place most rupture energy to the south of or under the peninsula are

574 not consistent with the tsunami data. The tsunami, rather than being unusually small for its generating earthquake's

575 moment magnitude (Sohn, 1998), generated runup averaging 6 m over about 60 km of coastline, and 30 cm

576 amplitude on the Hilo tide gage, requiring a "normal" offshore, subduction-zone rupture under a substantial depth of

577 water. Some significant portion of that rupture must be under substantial water depth to produce the indicated

578 tsunami north of Kronotsky Cape, while not generating as much runup on the Cape, or to the south. While part of

579 the rupture could well have been under the Kronotsky Peninsula and the relatively shallow region directly offshore,

580 deformation in deeper water east and north of the peninsula is needed.

581   We conclude that a rupture consistent with the mainshock and aftershock locations from Kamchatka's

582 network are more reasonable than more westerly locations, e.g., in the ISC catalogue (Fig. 2, Table S2). This issue

583 is illustrated by Hayes (2017) inversion, which takes the NEIC hypocentral location (Table S2) to start and, while

584 his inversion results in most slip to the north (Fig. S9), locates that slip under the peninsula, where it cannot generate

585 a tsunami.

586   The northern part of the Kamchatka subduction zone ruptured in two large events in February 1923 and

587 April 1923 (Fig. 1), and our study requires that a substantial portion of the energy released by the 1997 Kronotsky

588 earthquake was generated in a seismic gap between those earthquakes (Fig. 1), as originally recognized by Fedotov

589 et al. (1998) and predicted by his group's earlier work. The Kronotsky Peninsula lies landward of the (subducting)

590 Emperor Seamount chain, which has been postulated to generate an asperity and is characterized by a relatively

591 strong positive gravity anomaly (e.g., Bürgmann et al., 2005, Llenos and McGuire, 2007; Bassett and Watts, 2015)

592 (Fig. S9). That asperity may well keep the northern Kamchatka subduction zone from generating (Mw 9) 1952-

593 scale Kamchatka earthquakes, but it does rupture, as required by the tsunami data presented herein.

7.3 Paleotsunami results – implications for tectonic studies and hazard analyses

Southern Kamchatsky Bay has a relatively short but well-preserved record of paleotsunami deposits which can be calibrated with the historical record. Combined with the record in north Kamchatsky Bay (Pinegina et al., 2012) (the central bay is characterized by cliffs), the pattern of runup and inundation in the prehistoric record for the last 1700 years does not diverge from the 20th century record. Compared with southern Kamchatka, the region where Mw 9-scale events occurred in 1952 and 1737, the northern subduction zone has generated smaller and less extensive tsunamis, in agreement with analyses of Bürgmann et al. (2005) for the modern and Pinegina (2014) for the prehistoric record.

A robust, 1700-year-long record may be sufficient to generate a probabilistic hazard analysis that can be used for both local and far-field hazard studies, and not only for tsunami recurrence statistics, but also for recurrence statistics that include tsunami size. Reconstructing paleo- runup and paleo- inundation requires, and is thus limited by, accurate reconstructions of past shoreline locations and past (relative) sea levels. Coastlines with well-established marker tephra enable such reconstructions.

As are seismologists, paleoseismologists are cautioned by the lessons of the 11 March 2011 Tohoku earthquake and tsunami to qualify our generalizations. Characterizing subduction-zone behavior and quantifying its hazards are goals which we will only ever accomplish imperfectly.

Supplement link (will be included by Copernicus) – see supplemental material

Author contribution – we contributed equally and together

Competing interests -- none

Acknowledgments

Field research was supported by grants from the Russian Foundation for Fundamental Research (00-05-64697- to T.K. Pinegina), the National Geographic Foundation to Vera Ponomareva, and the U.S. National Science Foundation (EAR 9903341 to J. Bourgeois). Research and manuscript preparation were supported by RFBR grant 15-05-02651- to T. Pinegina and a U.S. Fulbright Foundation award to J. Bourgeois, which supported her visit to the Institute of Volcanology and Seismology, winter/spring of 2017.

We thank Vera Ponomareva for field advice and discussions regarding tephra stratigraphy and analysis; Alexander Lander for discussions concerning the nature of the 1997 Kronotsky earthquake; Alexander Gusev for discussions regarding the 1997 and earlier large earthquakes on Kamchatka; Vasily Titov for insights into the 1997 Kronotsky tsunami; and Vadim Saltykov for his helpful recommendations about statistical analyses of tsunami recurrence. We are grateful to Alexander Storcheus (deceased), Leonid Kotenko, Ivan Storcheus and Edward Cranswick for their field assistance. Roland Bürgmann, Andrea Llenos and Gavin Hayes offered helpful insights into their source models for 1997 Kronotsky.

References

Ammon, C. J., Kanamori, H. and Lay, T.: A great earthquake doublet and seismic stress transfer cycle in the central
Kuril islands, Nature 451.7178, 561-565, doi:10.1038/nature06521, 2008.

Balakina, L.M.: The October 4, 1994 Shikotan and December 5, 1997 Kronotsky earthquakes and their strongest
aftershocks as regular manifestations of the tectonic process in the Kuril-Kamchatka seismogenic zone,
Izvestiya - Russian Academy of Sciences, Physics of the Solid Earth, 36, 903-918, 2000.

Bassett, D. and Watts, A. B.: Gravity anomalies, crustal structure, and seismicity at subduction zones: 1. Seafloor
roughness and subducting relief, Geochemistry, Geophysics, Geosystems, 16, 1508-1540,
doi/10.1002/2014GC005684, 2015.

Bourgeois, J.: Geologic effects and records of tsunamis, Chapter 3 in The Sea, volume 15, Tsunamis, Harvard
University Press, 55-91, 2009.

Bourgeois, J., and Titov, V.V.: A Fresh Look at the 1997 Kronosky Tsunami, Transactions of the European
Geophysical Society, Abstracts, 2001.

Bourgeois, J., Pinegina, T., Ponomareva, V. and Zaretskaia, N.: Holocene tsunamis in the southwestern Bering Sea,
Russian Far East, and their tectonic implications, Geological Society of America Bulletin, 118, 449-463,
doi: 10.1130/B25726.1, 2006.

Braitseva, O.A., Ponomareva, V.V., Sulerzhitsky, L.D., Melekestsev, I.V. and Bailey, J.: Holocene key-marker
tephra layers in Kamchatka, Russia, Quaternary research, 47, 125-139, doi.org/10.1006/qres.1996.1876, 1997.

Bürgmann, R., Kogan, M.G., Levin, V.E., Scholz, C.H., King, R.W. and Steblov, G.M.: Rapid aseismic moment
release following the 5 December, 1997 Kronotsky, Kamchatka, earthquake, Geophys. Res. Lett., 28, 1331-
1334, doi: 10.1029/2000GL012350, 2001.

Bürgmann, R., Kogan, M.G., Steblov, G.M., Hilley, G., Levin, V.E. and Apel, E.: Interseismic coupling and
asperity distribution along the Kamchatka subduction zone, J. Geophys. Res., 110, B07405,
doi/10.1029/2005JB003648, 2005.

Fedotov, S.A., Chernyshev, S.D., Matviyenko, Y.D., and Zharinov, N.A.: Prediction of Kronotskoye earthquake of
December 5, 1997, M = 7.8-7.9, Kamchatka, and its strong aftershocks with M > or = 6, Volcanology and
Seismology, 6, 3-16, 1998, [in Russian].

Godzikovskaya, A.A.: Summary of macroseismic information on Kamchatka earthquakes (Pre-instrumental and
early instrumental observation period), Moskow – Petropavlovsk-Kamchatsky, 134 pp., 2010 [in Russian].

Gordeev, E.I., Ivanov, B.V. and Vikulin, A.V. (eds.): Kronotskoye earthquake of December 5, 1997 on Kamchatka,
Petropavlovsk-Kamchatsky, Kamchatkan State Academy of Fishing Marine, 294 pp., 1998, [in Russian with
English abstracts and figure captions].

Gordeev, E.I., Gusev, A.A., Levin, V.E., Bakhtiarov, V.F., Pavlov, V.M., Chebrov, V.N. and Kasahara, M.:
Preliminary analysis of deformation of the Eurasia-Pacific-North America plate junction from GPS data,
Geophys. J. Int., 147, 189-198, doi: https://doi.org/10.1046/j.0956-540x.2001.01515.x, 2001.

661   Gusev, A.A., Levina, V.I., Saltykov, V.A., and Gordeev, E.I.: Large Kronotskoye earthquake of Dec. 5, 1997: basic
662   data, seismicity of the epicentral zone, source mechanism, macroseismic effects, in Gordeev et al., eds., 32-54,
663   1998 [In Russian with English abstract and figure captions].

664   Gusev, A. A.: The schematic map of the source zones of large Kamchatka earthquakes of the instrumental epoch: in
665   Complex seismological and geophysical researches of Kamchatka. To 25th Anniversary of Kamchatkan
666   Experimental & Methodical Seismological Department, Ed. by Gordeev E.I., Chebrov V.N., Petropavlovsk-
667   Kamchatsky, 445 pp., 2004.

668   Gusev, A.A. and Shumilina, L.S.: Recurrence of Kamchatka strong earthquakes on a scale of moment magnitudes,
669   Izvestiya, Physics of the Solid Earth, 40, 206-215, 2004.

670   Hayes, Gavin P.: The finite, kinematic rupture properties of great-sized earthquakes since 1990, Earth and Planetary
671   Science Letters, 468, 94-100, doi: https://doi.org/10.1016/j.epsl.2017.04.003, 2017.

672   Kuzin, I.P., Levina, V.I., and Flenov, A.B.: Body wave velocity distribution in the Benioff zone of central
673   Kamchatka during aftershocks of the Kronotskii earthquake of 1997 (M = 7.9), J. Volcanology & Seismology,
674   1, 175-184, doi: 10.1134/S0742046307030037, 2007.

675   Kyle, P. R., Ponomareva, V. V., and Schluep, R. R.: Geochemical characterization of marker tephra layers from
676   major Holocene eruptions, Kamchatka Peninsula, Russia, International Geology Review, 53, 1059-1097,
677   http://dx.doi.org/10.1080/00206810903442162, 2011.

678   Leonov, V.L.: Ground ruptures, landslides and rockfalls caused by the earthquake on December 5, 1997 at the sea-
679   board of Kronotsky Peninsula: in Gordeev et al., eds., 240-246, 1998.

680   Levina, V. I., Lander, A. V., Mityushkina, S. V., and Chebrova, A. Y. The seismicity of the Kamchatka region:
681   1962–2011, Journal of Volcanology and Seismology, 7, 37-57, doi:10.1134/S0742046313010053, 2013.

682   Llenos, A. L., and McGuire, J. J.: Influence of fore ' arc structure on the extent of great subduction zone
683   earthquakes, Journal of Geophysical Research: Solid Earth, 112, B09301, doi:10.1029/2007JB004944, 2007.

684   Liu, P. L. F.: Tsunami modeling: propagation, The Sea, 15, 295-319, 2009.

685   MacInnes, B. T., Pinegina, T. K. Bourgeois, J, Razhigaeva, N, G., Kaistrenko, V. M., and Kravchunovskaya, E. A.:
686   Field survey and geological effects of the 15 November 2006 Kuril tsunami in the middle Kuril Islands:
687   In Tsunami Science Four Years after the 2004 Indian Ocean Tsunami, Birkhäuser Basel, 9-36, doi
688   10.1007/s00024-008-0428-3, 2009.

689   MacInnes, B.T., Weiss, R., Bourgeois, J. and Pinegina, T.K.: Slip distribution of the 1952 Kamchatka great
690   earthquake based on near-field tsunami deposits and historical records, Bulletin of the Seismological Society of
691   America, 100, 1695-1709, doi: 10.1785/0120090376, 2010.

692   MacInnes, B., Kravchunovskaya, E., Pinegina, T., and Bourgeois, J. Paleotsunamis from the central Kuril Islands
693   segment of the Japan-Kuril-Kamchatka subduction zone, Quaternary Research, 86, 54-66,
694   https://doi.org/10.1016/j.yqres.2016.03.005, 2016.

695   Martin, M. E., Weiss, R., Bourgeois, J., Pinegina, T. K, Houston, H. and Titov, V. V. Combining constraints from
696   tsunami modeling and sedimentology to untangle the 1969 Ozernoi and 1971 Kamchatskii tsunamis, Geophys.
697   Res. Lett., 35, L01610, doi:10.1029/2007GL032349, 2008.

698   Melekestsev, I.V, Braitseva, O.A., Erlikh, E.N., Shantser, A.E., Chelebaeva, A.I., Lupikina E.G., Egorova, I.A.,
699   Kozhemyaka, N.N.: Kamchatka, Komandor and Kurile Islands, Moskow, Nauka, 439 pp., 1974 [in Russian].
700   Nanayama, F., Furukawa, R., Shigeno, K., Makino, A., Soeda, Y. and Igarashi, Y.: Nine unusually large tsunami
701   deposits from the past 4000 years at Kiritappu marsh along the southern Kuril Trench, Sedimentary
702   Geology, 200, 275-294, https://doi.org/10.1016/j.sedgeo.2007.01.008, 2007.
703   NCEI, National Centers for Environmental Information (formerly NGDC), Natural Hazards Data, Images and
704   Education, Tsunami and Earthquake databases: https://www.ngdc.noaa.gov/hazard/hazards.shtml
705   Okal, E.A. and Synolakis, C.E.: Source discriminants for near-field tsunamis, Geophysical Journal International, 158,
706   899-912, DOI: https://doi.org/10.1111/j.1365-246X.2004.02347.x, 2004.
707   Petukhin, A.G., Dontsov, O.V., Kozlov, V.N., and Sinitsyn, V.I.: Preliminary analysis of strong ground-motion
708   records of the Kronotskoye earthquake of December 5, 1997 (Mw = 7.9): in Gordeev et al., eds., 247-256, 1998,
709   [In Russian with English abstract and figure captions].
710   Pinegina T. K.: Time-space distribution of tsunamigenic earthquakes along the Pacific and Bering coasts of
711   Kamchatka: insight from paleotsunami deposits, Doctor of Geological Science dissertation, Institute of
712   Oceanology RAS, Moscow, 235 pp., 2014 [in Russian].
713   Pinegina, T. K., Kozhurin, A. I., Ponomareva, V. V.: Seismic and tsunami hazard assessment for Ust-Kamchatsk
714   settlement, Kamchatka, based on paleoseismological data, Bulletin of Kamchatka regional association
715   "Educational-scientific center". Earth sciences. 1, 138-159, 2012 [in Russian with English abstract].
716   Pinegina, T.K., Bourgeois, J., Kravchunovskaya, E.A., Lander, A.V., Arcos, M.E., Pedoja, K. and MacInnes, B.T.:
717   A nexus of plate interaction: Vertical deformation of Holocene wave-built terraces on the Kamchatsky
718   Peninsula (Kamchatka, Russia), Geological Society of America Bulletin, 125, 1554-1568,
719   doi: 10.1130/B30793.1, 2013.
720   Ponomareva, V., Portnyagin, M., Pendea, I.F., Zelenin, E., Bourgeois, J., Pinegina, T., and Kozhurin A. A.: A full
721   Holocene tephrochronology for the Kamchatsky Peninsula region: applications from Kamchatka to North
722   America, Quaternary Science Reviews, 2017 [in press].
723   Slavina, L.B., Pivovarova, N.B. and Levina, V.I.: A study in the velocity structure of December 5, 1997, Mw = 7.8
724   Kronotskii rupture zone, Kamchatka, J. Volcanology & Seismology, 1, 254-262,
725   doi:10.1134/S0742046307040045, 2007.
726   Sohn, S.W.: The 1997 Kamchatka earthquake. Individual Studies by Participants at the International Institute of
727   Seismology and Earthquake Engineering, Tokyo, International, 34, 91-99,1998.
728   Song, T. R. A. and Simons, M.: Large trench-parallel gravity variations predict seismogenic behavior in subduction
729   zones, Science, 301, 630-633, DOI: 10.1126/science.1085557, 2003.
730   Zayakin, Yu. A. and Luchinina, A.A.: Catalogue tsunamis on Kamchatka, Obninsk: Vniigmi-Mtsd, 51pp., 1987,
731   [Booklet in Russian].
732   Zayakin, Yu. A. and Pinegina, T.K.: Tsunami in Kamchatka on December 5, 1997: in Gordeev et al., eds., 257-263,
733   1998, [In Russian with English abstract and figure captions].

734   Zobin, V.M. and Levina, V.I.: The rupture process of the Mw 7.8 Cape Kronotsky, Kamchatka, earthquake of 5

735   December 1997 and its relationship to foreshocks and aftershocks, Bull. Seis. Soc. Am., 91, 1619-1628,

736   doi: 10.1785/0119990116, 2001.